JOURNAL OF
Materials
CHEMISTRY

Sonochemical synthesis of tungsten sulfide nanorods†

Sergei I. Nikitenko,[a] Yuri Koltypin,[b] Yitzhak Mastai,[c] Maxim Koltypin[b] and Aharon Gedanken*[b]

[a]*Institute of Physical Chemistry, RAS, Leninskii Pr.31, Moscow Russia*
[b]*Department of Chemistry, Bar-Ilan University, Ramat-Gan, Israel.*
E-mail: gedanken@mail.biu.ac.il.; Fax: +972-3-535-1250; Tel: +972-3-531-8315
[c]*Max Planck Institute of Colloids and Interfaces, Golm, Germany*

Received 27th November 2001, Accepted 26th February 2002

Amorphous WS_2 has been prepared by ultrasound irradiation of $W(CO)_6$ solution in diphenylmethane (DPhM) in the presence of a slight excess of sulfur at 90 °C under argon. Heating the amorphous powder at 800 °C under argon yields WS_2 nanorods and their packings. The average size of WS_2 nanorods was found to be 3–10 nm and 1–5 µm in thickness and length, respectively. The prepared WS_2 has been characterized by elemental analysis, X-ray powder diffraction measurements, FTIR spectroscopy, differential scanning calorimetry, thermogravimetric analysis, transmission electron microscopy, scanning electron microscopy, atomic force microscopy and energy dispersive X-ray analysis.

Introduction

There is considerable interest in the development of new synthetic routes to WS_2 nanoparticles, because of their novel and superior properties when compared with bulk WS_2. So, it has been shown that WS_2 nanoparticles possess enhanced catalytic activity,[1] photoconductivity,[2] and excellent tribological properties.[3] Recently WS_2 nanotubes and fullerene-like nanocrystals have been prepared.[4] WS_2 nanotubes have been tested successfully as tips in scanning probe microscopy.[5] Most of these unusual and useful properties of WS_2 arise from the high degree of anisotropy associated with its crystal structure. WS_2 crystallizes into a layered structure, in which atoms forming each layer are covalently bonded while adjacent layers are held weakly by van der Waals forces. For instance, the weak binding between layers in the basal planes leads to the useful lubrication properties of WS_2. It should be noted that the utility of WS_2 and other layered materials such as MoS_2 depends strongly on their crystallographic orientation, namely, crystal morphology and crystal sizes.

Nanostructured WS_2 is usually prepared by the reaction of WO_x with H_2S at high temperature,[4] a microwave plasma process from $W(CO)_6$ and H_2S,[6] thermolysis of tetraalkylammonium thiotungstates,[7] heating of amorphous W with $H_2S–N_2H_2$ gaseous mixture,[8] and nitric acid treatment of commercial WS_2 sample followed by heating under vacuum.[9]

Sonochemical reaction of volatile metal carbonyls is a relatively new method for the synthesis of nanophased materials. These reactions were developed by Suslick and co-workers.[10] The extremely high temperatures ($\sim$5000 K), pressures (>20 MPa) and cooling rates ($>10^9$ K s^{-1}) attained during acoustic cavitation within the collapsing bubbles lead to many unique properties in the irradiated solution. These extreme conditions have been exploited to decompose the metal–carbonyl bonds and generate nanoparticles, such as nanosized metals, metal oxides and metal carbides.[10] Recently a highly effective catalyst based on nanosized MoS_2 was prepared by sonication of $Mo(CO)_6$ and S in isodurene (1,2,3,5-tetramethylbenzene) under Ar.[11] The sonochemical synthesis of nanosized WS_2 has not been performed until this time due to the extremely low solubility of $W(CO)_6$ in hydrocarbons. We report here a simple and effective method for the synthesis of WS_2 nanorods based on the sonochemical reaction of $W(CO)_6$ in diphenylmethane (DPhM) in the presence of sulfur followed by the thermal treatment of as-prepared material.

Experimental

Diphenylmethane (>99%, Fluka) and $W(CO)_6$ (97%, Aldrich) were used without additional purification. 12 mmol of $W(CO)_6$ and 26 mmol of S were dissolved in 80 cm^3 of DPhM under heating in an argon flow. The solution was sonicated for 3 h. under argon. Ultrasonic irradiation was accomplished with a high-intensity ultrasonic probe (Sonics&Materials VCX 600 Sonifier, 1 cm^2 titanium horn, 20 kHz, 40 W cm^{-1}). Temperature during sonication was kept at 90 °C. The black solid product was removed by centrifugation, washed with toluene and twice with dry pentane inside a N_2-filled glove-box and dried under vacuum at room temperature.

Elemental analysis of the prepared material was carried out by an Eager 200 CHNS Analyzer. X-Ray diffractograms (XRD) were collected by employing a Bruker AXS D* Advance Powder X-Ray Diffractometer (Cu-Kα radiation, λ = 1.5418 Å). Energy dispersive X-ray analysis (EDX) was conducted using an X-ray microanalyzer (Oxford Scientific) attached to a JSM-840 Scanning Electron Microscope (SEM). The transmission electron micrographs (TEM) were obtained on a JEOL-JEM 100SX microscope, working at 100 kV acceleration voltage. High resolution TEM images were obtained by employing a JEOL-3010 with 300 kV accelerating voltage. Samples for TEM were prepared by placing a drop of the sample suspension on a copper grid coated with a carbon film and were allowed to dry in air. Atomic force microscopic measurements (AFM) were obtained by a Topometrix microscope in contact mode using a 70 µm scanner. The thermogravimetric analysis (TGA) and differential scanning calorimetric measurements (DSC) were performed by using Mettler Toledo TGA/SDTA 851 and DSC-25/TC-15 devices, respectively, under nitrogen flow. FTIR spectra were recorded in KBr pellets using an Impact 410 Nicolet spectrometer.

---

†Electronic supplementary information (ESI) available: TGA curve for the as-prepared product; AFM image of WS_2 packs of nanorods. See http://www.rsc.org/suppdata/jm/b1/b110867k/

DOI: 10.1039/b110867k

Results and discussion

Elemental and EDX analysis

The initially yellow color of the solution changes to black under sonication. 1.1 g of the black solid is removed from the sonicated solution after centrifugation. CNHS elemental analysis shows that as-prepared material contains 16.1 wt% of carbon, 2.2 wt% of hydrogen, and 23.9 wt% of sulfur. Most probably, carbon and hydrogen come from the sonication product of DPhM. In fact, the sonolysis of neat DPhM yields a black solid, which is characterized as a sonopolymer. Since elemental sulfur is well soluble in DPhM its presence in the precipitate indicates that tungsten sulfide is formed in the sonochemical stage. After annealing at 600 °C in Ar flow for 12 hours, the majority of C and H disappears, but the CHNS analysis still indicates the presence 0.3 wt% of carbon and 24.9 wt% of sulfur in the product. The sulfur content corresponds well to the WS_2 stoichiometry (25.8 wt%) after annealing. EDX measurements of as-prepared and annealed samples indicate the presence of W and S in the atomic ratio 1 : 2.9 and 1 : 2.2 respectively.

FTIR, TGA, DSC and XRD studies

FTIR spectra of the as-prepared product reveal the presence of absorption bands at 3060–3020 cm^{-1} and 2900–2850 cm^{-1} assigned to C–H stretching vibrations in aromatic and aliphatic groups, respectively.[12] Most probably, these bands are related to the polymer formed from DPhM. Annealing causes their disappearance in agreement with the elemental analysis data.

The TGA curve of the as-prepared product (see ESI†) reveals 16.9 wt% mass loss in the temperature range 200–500 °C. The DSC curve exhibits several broad and relatively small thermal effects in the temperature range of 200–550 °C, which can be attributed to the thermal destruction of the organic polymer. A sharp exothermic peak characteristic for WS_2 crystallization process is not observed in the studied temperature range.

The as-prepared product and sample annealed at 600 °C are X-ray amorphous as follows from XRD patterns shown in Fig. 1a,b. To prepare crystalline WS_2 the amorphous sample preheated at 600 °C was annealed in pure argon ($\sim$0.3 ppm O_2) at 800 °C for at least 12 hours. XRD patterns of the annealed sample presented in Fig. 1c clearly indicate the formation of crystalline tungstenite WS_2 (X-ray diffraction file N 08-0237). Some admixture of orthorhombic WO_2 is also presented according to XRD (X-ray diffraction file N 82-728).

SEM, AFM and TEM measurements

Fig. 2 displays the SEM image of the annealed sample; showing that micrometre rod-like crystal morphology dominates. Low-resolution TEM images of the as-prepared and annealed materials are presented in Fig. 3a,b, respectively. The as-prepared X-ray amorphous material has a globular morphology, whereas the annealed crystalline WS_2 consists of 3–10 nm diameter nanorods up to 1 μm in length. However it should be noted that, beside the dominant rod-like crystal morphology, spherical crystals with a typical size of *ca.* 100 nm are also observed in the annealed samples. The high resolution TEM picture of the rod-like crystal morphology is shown in Fig. 4. It reveals a layer structure with lattice fringes (interlayer spacing) of 0.599 nm, corresponding to the 002 plane of conventional WS_2 (X-ray diffraction file N 08-0237). It is important to point out that commercial bulk WS_2 shows a plate-like morphology,[9] in comparison with the rod-like shape observed in our samples. AFM measurements (ESI†) reveal that microscopic WS_2 rods exist as packing of nanosized rods.

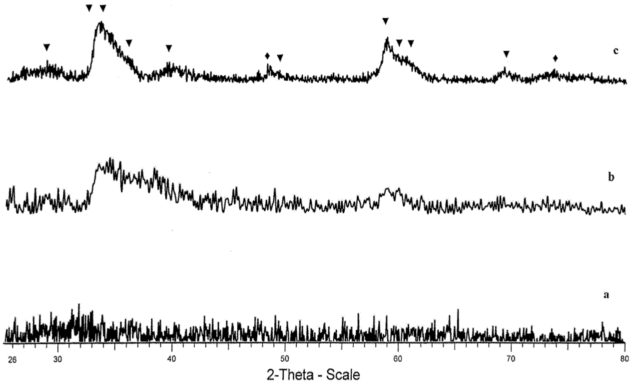

Fig. 1 XRD patterns for as-prepared product (a), heated at 600 °C (b) and annealed 800 °C (c), (▼) WS_2, (⧫) WO_2.

Fig. 2 SEM image of WS_2 nanorods and packs of nanorods.

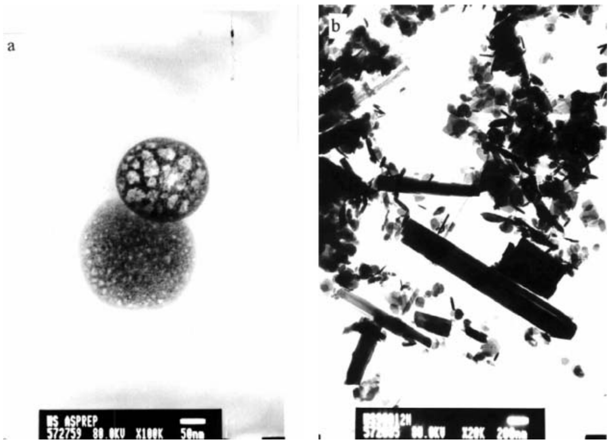

Fig. 3 Low resolution TEM image of as-prepared material (a) and WS_2 annealed at 800 °C (b).

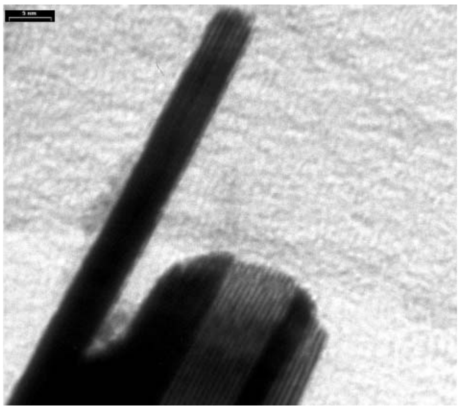

Fig. 4 High resolution TEM image of WS_2 nanorods. Scale bar: 5 nm.

Probable mechanism of WS_2 nanorods formation

The data obtained clearly indicate that WS_2 is formed at the stage of $W(CO)_6$ sonolysis. Most probably, the decomposition of $W(CO)_6$ is the primary stage of the process taking place in the gaseous phase of the cavitating bubble:

$$W(CO)_6\ ))) \rightarrow W + 6CO \qquad (1)$$

where the symbol))) corresponds to the high temperature process inside the cavitating bubble. It is known that sonolysis of $Mo(CO)_6$ in hydrocarbons causes tungsten carbide formation.[13] It can be assumed that sonochemical decomposition of $W(CO)_6$ also should yield tungsten carbide in the solutions of DPhM. However WS_2 is formed in the presence of elemental sulfur since tungsten sulfide is thermodynamically more stable than tungsten carbide ($\Delta H^{\circ}_{f} = -49$ kcal mol^{-1} and $+7.1$ kcal mol^{-1} for WS_2 and W_2C respectively).[14] MoS_2 is formed sonochemically due to similar reasons in isodurene in the presence of sulfur.[11]

In our experiments WS_2 is not formed as nanotubes unlike other recent works.[4–9] The folding of WS_2 into a nanotube structure reported in other work, is commonly explained by analogy to the formation of carbon-based fullerenes, that is to say due to building of the two-dimensional WS_2 layers into the closed nanotube structure.

It can be assumed that the polymer formed during DPhM sonication plays an important role in the particle's morphology. It is well known[15] that the presence of impurities, especially high molecular impurities such as polymers, can alter the shape of a growing crystal. As a rule it is assumed that polymeric impurities modify the crystal shape by specific binding to different growing crystal faces. In our case the sonolysis of $W(CO)_6$ occurs simultaneously with DPhM sonochemical decomposition. Therefore, the formed WS_2 at the sonochemical stage is co-precipitated with the sonopolymer. Fig. 4a shows a typical nanoglobule composite structure, where very small dense WS_2 particles are dispersed in a polymer matrix. Annealing of the nanocomposite causes agglomeration of the WS_2 particles and, then, their crystallization. It can be assumed that the products of the sonopolymer destruction coat the WS_2 agglomerates at the initial stage of crystallization and thus avoid rolling of WS_2 layered particles into nanotubes. The rod-like shape observed in our WS_2 crystals is probably due to specific interactions of the sonopolymer with different WS_2 crystal faces. There are few studies[16,17] in which rod-like WS_2 crystals were reported mainly for chemical vapor deposition (CVD) of thin WS_2 films on to well defined substrata such as Si (1 0 0). In those studies the rod-like crystal shape is explained due to high growth rate in the basal direction of WS_2. In a similar manner it can be assumed that the sonopolymer kinetically facilitates the preferred growth of WS_2 into rod-like shapes *via* strong interactions with the crystal faces in the basal crystal direction of WS_2.

Conclusions

Nanosized WS_2 has been prepared for the first time using sonolysis of $W(CO)_6$ in diphenylmethane in the presence of sulfur at moderate temperature.

Annealing of amorphous sample at 800 °C in pure argon yields WS_2 nanorods of 3–10 nm in thickness and 1–5 μm in length. Nanorods form packs in the micrometre size range.

Acknowledgement

S. I. Nikitenko thanks the Bar-Ilan Research Authority for his fellowship. A. Gedanken is grateful for the support of the German Ministry of Science through the Deutsche-Israeli DIP program. Yu. Koltypin thanks the Ministry of Absorption, the Center for Absorption in Science, for the financial support. The authors also thank Dr Shifra Hochberg for editorial assistance.

References

1 *Advanced Catalysts and Nanostructured Materials*, ed. W. R. Moser, Academic Press, New York, 1996.
2 C. Ballif, M. Regula and F. Levy, *Sol. Energy Mater. Sol. Cells*, 1999, **57**, 189.
3 Y. Feldman, A. Zak, R. Popovitz-Biro and R. Tenne, *Solid State Sci.*, 2000, **6**, 663.
4 R. Tenne, L. Margulis, M. Genut and M. Hodes, *Nature*, 1992, **360**, 444; R. Tenne, L. Margulis and G. Hodes, *Adv. Mater.*, 1993, **5**, 386; Y. Feldman, G. L. Frey, M. Homyonfer, V. Lyakhovitskaya, L. Margulis, G. Cohen, G. Hodes, J. L. Hutchison and R. Tenne, *J. Am. Chem. Soc.*, 1996, **118**, 5362; A. Rothschild, J. Sloan and R. Tenne, *J. Am. Chem. Soc.*, 2000, **122**, 5169; Y. Q. Zhu, W. K. Hsu, H. Terrones, N. Grobert, B. H. Chang, M. Terrones, B. Q. Wei, H. W. Kroto, D. R. M. Walton, C. B. Boothzoyd, I. Kinloch, G. Z. Chen, A. H. Windle and D. J. Fray, *J. Mater. Chem.*, 2000, **10**, 2570; Y. Q. Zhu, W. K. Hsu, N. Grobert, B. H. Chang, M. Terrones, H. Terrones, H. W. Kroto and D. R. M. Walton, *Chem. Mater.*, 2000, **12**, 1190.
5 A. Rothschild, S. R. Cohen and R. Tenne, *Appl. Phys.Lett.*, 1999, **75**, 4025.
6 D. Vollath and D. V. Szalo, *Mater. Lett.*, 1998, **35**, 236.
7 G. Alonso, M. Del Valle, J. Cruz, A. Licea-Claverie, V. Petranovskii and S. Fuentes, *Catal. Lett.*, 1998, **52**, 55; G. Alonso, V. Petranovskii, M. Del Valle, J. Cruz-Reyes, A. Licea-Claverie and S. Fuentes, *Appl. Catal. A*, 2000, **197**, 87.
8 L. Margulis, R. Tenne and S. Iijima, *Microsc. Microanal. Microstruct.*, 1996, **7**, 87.
9 E. B. Mackie, D. H. Galvan, E. Adem, S. Talapatra, G. Yang and A. D. Migone, *Adv. Mater.*, 2000, **12**, 495.
10 K. S. Suslick, S. B. Choe, A. A. Cichowlas and M. W. Grinstaff, *Nature*, 1991, **353**, 414.
11 M. M. Mdleleni, T. Hyeon and K. S. Suslick, *J. Am. Chem. Soc.*, 1998, **120**, 6189; N. A. Dhas, A. Ekhtiarzadeh and K. S. Suslick, *J. Am. Chem. Soc.*, 2001, **123**, 8310.
12 K. Nakanishi and P. H. Solomon, *Infrared Absorption Spectroscopy*, Holden-Day, Inc., San Francisco, 1982.
13 T. H. Hyeon, M. M. Fang and K. S. Suslick, *J. Am. Chem. Soc.*, 1996, **118**, 5492.
14 *Comprehensive Inorganic Chemistry*, ed. J. C. Bailar, Pergamon Press, New York, 1973.
15 A. Mersmann, *Crystallization Technology Handbook*, Marcel Dekker, New York, 2001.
16 J. W. Chung, Z. R. Dai and F. S. Ohuchi, *J. Cryst. Growth*, 1998, **186**, 137.
17 A. Ennaoui, S. Fiechter, K. Ellmer, R. Scheer and K. Diesner, *Thin Solid Films*, 1995, **261**, 124.